Strength evaluation of continuous curvilinear variable stiffness panels with circular cut-outs under biaxial normal loading and off-design conditions

Mahdi Arian Nik[1], Kazem Fayazbakhsh[2]*, Sadben Khan[2], Zouheir Fawaz[2],

[1]*Department of Mechanical Engineering, McGill University, Macdonald Engineering Building, 817 Sherbrooke West, Montreal, QC, Canada H3A 2K6*

[2]*Aerospace Engineering Department, Ryerson University, 350 Victoria Street, Toronto, ON, Canada M5B 2K3*

**Corresponding author: kazem@ryerson.ca; Tel: (+1) 416-979-5000 ext. 6414; fax: (+1) 416-979-5056*

Abstract

Continuous curvilinear variable stiffness (CCVS) design is explored to improve strength of panels with cut-outs compared to straight-fiber laminates. All possible biaxial loading combinations and several force ratios are investigated. A total of 40 optimization problems (40 loading conditions) are solved using a surrogate-based genetic algorithm. CCVS designs provide at least 50 % improvement in failure load for all loading conditions over a quasi-isotropic laminate, the baseline. Under off-design conditions, some CCVS designs outperform the baseline for all loading conditions by an average of 52 % and 44 %, respectively, for a plate with a small and a large hole.

Keywords:

Continuous curvilinear variable stiffness (CCVS) design; biaxial normal loading; off-design condition; optimization; Composites; Strength.

Mechanics of Advanced Materials and Structures

https://doi.org/10.1080/15376494.2021.1912441

1. Introduction

Efficiency and weight reduction have been major design goals for modern aerospace structures to alleviate carbon emissions and reduce operation cost. As a result, many designs have utilized optimization techniques to tailor structures to their peak efficiency. Composite laminates benefit greatly from optimization as innovations in advanced manufacturing techniques, e.g., automated fiber placement (AFP), have allowed for precise placement of fibers along prescribed paths using robotic or gantry-based systems. Using AFP technology, fibers can follow curvilinear paths and composite laminates are no longer limited to straight-fiber paths used in traditional designs. Curvilinear fiber paths allow for the stiffness of a structure to vary spatially resulting in a variable stiffness (VS) design. The introduction of the VS design results in structures with unique characteristics, like decoupling of stiffness and buckling load as well as significantly improving their load carrying capacity [1]. An interesting property of laminates utilizing a VS design, is the capability of the loads to be distributed across the panel. This concept can be used to improve the performance of structures featuring large cut-outs, as these discontinuities are significant stress concentration regions. Typically, these areas are reinforced with doublers or thickness built-up that resist the higher stresses [2].

Jegley et al. [3] optimized panels with circular cut-outs using a VS design to reduce the stress concentration around the hole, thereby increasing their load carrying capacity. They optimized panels for buckling load using an in-house laminate design tool based on genetic algorithms. Experimentally determined buckling and failure loads of the VS panel with a large hole and overlap pattern were 89 % and 55 % higher compared to a straight-fiber laminate, respectively. Non-Circular cut-outs were examined by Wu et al. [4], where a variable stiffness cylinder with an ovoid fuselage cut-out was subjected to axial compression. Two cylinders of identical layups were compared, one with no cut-out and the second one with an ovoid cut-out. The cylinder with a cut-out was able to maintain 91 % of the axial stiffness and 85 % of the buckling load when compared to the cylinder with no cut-out. Large deflections where measured radially outward in the cut-out region and there was no baseline quasi-isotropic laminate comparison. Alhajamad et al. [5] further investigated mechanical performance of VS designs for a fuselage with ovoid cut-outs. They explored the buckling and first ply failure of a fuselage undergoing internal pressure and shear loading. Finite element analysis (FEA) was conducted in ABAQUS and the results showed that

the VS design did not improve the load carrying capacity compared to a quasi-isotropic laminate. Lopes et al. [6] optimized VS panels with a circular cut-out for buckling and first-ply failure in the post-buckling regime separately, and compared results with straight-fiber designs. They found a buckling performance ratio of 2.39 between the ideal VS design and the optimum straight-fiber laminate. Unlike buckling performance, there was only 20.6 % improvement in first-ply failure load for the ideal VS design compared to the optimum straight-fiber configuration. To ensure manufacturability, researchers in the previously mentioned studies [3-6] assumed a fiber path formulation, e.g., linear fiber angle variation, and found optimum variable stiffness panels. As a result, the design space for VS panels was limited and the fiber paths were broken at the cut-out boundary.

Steering fibers around discontinuities has shown promising improvements in VS design of composite components by reducing stress concentration around cut-outs. Several techniques have been developed experimentally and numerically to find optimum curvilinear fiber paths. An example of an experimental technique was first demonstrated by Yau and Chou [7], who steered fibers around holes by inserting metal pins into woven fabric prior to curing. The resulting molded-in laminate was shown to have a marked improvement over the one with drilled holes in tension and compression. A similar technique was utilized in a study conducted by Durante and Langella [8], where an improvement of 15 % in bearing strength was found when the tows were steered around a pin, but the complex manufacturing method and variation in results reduce the practicality. Furthermore, a major concern with the pin technique is the resulting large gap around the hole leading to complex laminate behavior that cannot be accurately predicted. Numerical investigation was led by Hyer and Lee [9], in which they used a gradient search and sensitivity analysis techniques with finite element method (FEM) to improve buckling performance of a plate with centrally located circular cut-out undergoing compression loading. A significant improvement in the buckling load was observed, but the resulting design was not manufacturable. Similarly, Huang and Haftka [10] repeated the study with a tension loading and a similar optimization approach. The results showed that the fiber angles follow a concentric path around the hole, while tending to the far-field loading directions away from it. Furthermore, a study on bolted composites by Gustafson [11] using FEM showed that aligning fibers along the principal stress directions can improve the failure load by 36 % to 64 % over a quasi-Isotropic laminate

dependent on the number of bolt holes. The resulting streamline plot of the fiber paths showed that they tended to continuously curve around the bolted regions. Montemurruo and Catapano [12] used a B-Spline and genetic algorithm approach to optimize a panel with a centrally located circular cut-out undergoing a biaxial tension loading which resulted in a 12 % improvement in stiffness over the optimum straight-fibre counterpart. In a follow-up study, Catapano and Montemurro [13] used the laminate failure criteria presented in [14] and formulated the strength optimization of variable stiffness plates with a central hole subjected to feasibility constraints on the laminate polar parameters and minimum allowable turning radius. The results of the most optimal layup showed that the fiber directions tended to curve around the cut-out as well. Shafigfard et al. [15] also investigated circular and ovoid cut-outs as well as cut-outs of non-conventional geometry. They used a three-level scheme including lamination parameter, direct search method, Least Squares, and continuity constraint method (LSC) to optimize the fiber angles for minimum strain energy/compliance. The fibers tended to bend around the circular cut-out and showed a significant improvement of 45.8 % in compliance relative to the optimum constant stiffness design.

Most researchers who worked on the design and analysis of VS panels investigated uniaxial loading since they were able to later manufacture and validate their results experimentally with relative ease. Unlike uniaxial testing machines that are available in many research laboratories, biaxial testing equipment is expensive and limited to a handful of universities. All research studies discussed previously except for the work of Montemurruo and Catapano [12, 13] and Shafigfard et al. [15] explored uniaxial loading. Montemurruo and Catapano [12, 13] considered the case study proposed by Catapano et al. [16] and explored biaxial tension loading with force ratios of $F_y/F_x = 0.5$ and 1. Shafigfard et al. [15] also investigated biaxial tension loading, but considered two force ratios of $F_y/F_x = 1$ and 2 [13]. As previously mentioned, under these biaxial loading cases, researchers still found improvements in structural performance of the optimum VS panels compared to the straight-fiber counterparts [12, 13, 15]. While interesting, these research studies did not investigate structural performance of VS panels under all possible combinations of biaxial loading (e.g., tension-compression) and/or various force ratios.

All previously discussed research work optimized a structure for a loading condition and found significant improvements in structural performance using VS design concept compared to CS laminates. It should be noted that a part might undergo a loading which does not correspond exactly to the one used during the design and optimization stages (off-design conditions). Huang and Haftka [10] proposed the addition of ±45° layers to a variable stiffness layup to offer robustness under off-design conditions. They considered symmetric six-layer [(C-0)/±45]s and $[C\text{-}0]_6$ plates with a central hole. The C-0 represents a variable stiffness layer, where the fiber orientation can vary discretely near the hole and is fixed at 0° away from the hole. As expected, improvements in load carrying capacity from optimized variable stiffness design over the baseline laminate, [0/+45/-45]s, was lower for [(C-0)/±45]s compared with $[C\text{-}0]_6$ (88 % versus 100 %). Furthermore, an optimized VS design may not yield favorable results when there is a change in loading direction and/or scenario. Rouhi et al. [15] optimized a VS composite cylinder for improved buckling load under unidirectional bending along the center line. The results indicated a significant improvement of 25 % over a quasi-isotropic laminate; however, there was a reduction in the buckling load of 57 % when the bending load was applied in the opposite direction. Jegley et al. [18] also investigated off-design loads by subjecting their open hole panel to a shear load when the panel was previously optimized for a uniaxial compression. The results indicated that there was little improvement in the buckling load compared to a CS design, while there was still approximately a 14 % improvement in the ultimate failure load. Gomes et al. [19] further investigated the centrally located circular cut-out of a panel using a VS design based on the work of Jegley et al. [18]. They found a mismatch between the optimal VS panels for compressive and shear loads.

Although performance improvements of VS over CS designs are significant and show a promising avenue for industrial applications, these improvements might be limited under biaxial loading and/or off-design conditions. While limited research work on bi-axial loading of VS laminates exists in the literature [12, 13, 15], they did not investigate all possible biaxial loading combinations, e.g. tension-compression. They also explored a limited number of force ratios, i.e., a maximum of two for the work of Catapano and Montemurro [13], and Shafigfard et al. [15]. Furthermore, performance of the optimized laminates under off-design conditions were not explored, which reduces their appeal for real world applications. Here, we explore a square plate with a central hole under all possible combinations of bi-axial normal loading and their force ratios

(a total of 40 loading conditions). In addition, for any optimized laminate, its performance is evaluated under all the other loading conditions, resulting in 39 off-design conditions. Therefore, a comprehensive overview of VS design performance over CS design is presented, which motivates its use in industrial applications.

In this paper, MATLAB subroutines are developed to generate the fiber paths per continuous curvilinear variable stiffness (CCVS) design [20, 21]. Then, the fiber angles are passed to a FEA code in Nastran to evaluate failure indices for all designs. A surrogated-based genetic algorithm (GA) determines the optimum trajectories to maximize load carrying capacity under biaxial normal loading. Then, structural performance of the optimum designs is evaluated for all off-design conditions and is compared with a quasi-isotropic laminate as the baseline.

2. Methodology

2.1. Case study

A square plate (L = W = 14 in or 0.356 m) with a circular hole located at its center is considered as the case study. The plate dimensions are representative of real-world applications and is large enough to obtain improvements from fiber steering. Two hole diameters (D) are considered leading to W/D =2 (hole diameter of 7 in or 17.8 cm) and W/D=4 (hole diameter of 3.5 in or 8.89 cm). Loading along x and y are denoted by F_x and F_y, respectively (Figure 1a). The ratio between F_y and F_x can be represented by angle β (Eq.1). In addition, an equivalent load, F_{eq}, is defined for the biaxial loading condition (Eq. 2).

$$\beta = \tan^{-1}\left(\frac{F_y}{F_x}\right) \tag{1}$$

$$F_{eq} = \sqrt{{F_x}^2 + {F_y}^2} \tag{2}$$

By changing the angle β from 0° to 360°, it is possible to investigate all combinations of biaxial normal loading, i.e., tension-tension (T-T), compression-tension (C-T), compression-compression (C-C), and tension-compression (T-C), and their force ratios (Figure 1b). Regarding boundary conditions, all the exterior edges are constrained with simply supported boundary conditions while the internal hole boundary is considered free. This means that while loading is applied on the plate exterior edges, the displacement along all of them will be uniform, which simulates biaxial

experimental testing. In addition, these boundary conditions were used by other researchers in the modeling of a window opening in a pressurized fuselage skin as a plate with a central cut-out [5].

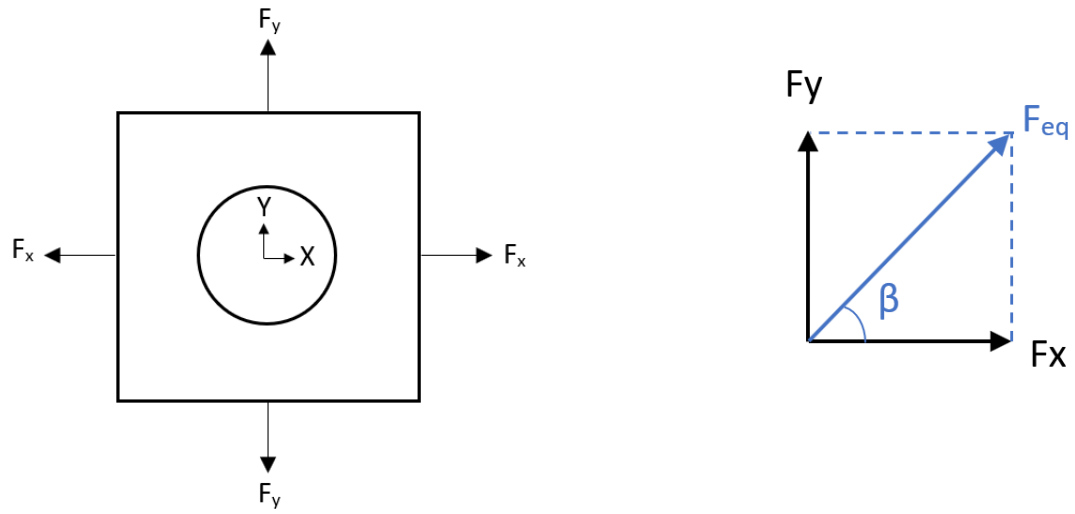

(a) **(b)**

Figure 1. Case study: (a) a square plate with a central cut-out including biaxial loading conditions; and (b) biaxial loading ratio represented with angle β.

In this study, β is varied in 10-degree increments with β = 45°, 135°, 225°, and 315° also added to the list (a total of 40 angles) to study the special cases of equi-biaxial load ratios. When β = 0°, the case study is a uniaxial tensile loading along x and by increasing β up to 90°, it changes to biaxial tension loading with a force ratio (F_y/F_x) of less than one (1) for all β < 45° and more than one (1) for all β > 45°. At angles close to 0° and 90°, the case study is under a uniaxially dominant load along x and y, respectively. This representation still holds for other quadrants knowing that the combination of biaxial normal loading is different, i.e., 90° < β < 180°: C-T, 180° < β < 270°: C-C, and 270 < β < 360: T-C.

The square plate is a 16-ply symmetric balanced laminate with a variable-stiffness layup $<\pm T_1/\pm T_2/\pm T_3/\pm T_4>_s$. It should be noted that the symmetric and balanced stacking sequence assumption shrinks the design space. However, it ensures no warping, and normal and shear coupling in the fabricated plates, which are required for many industrial applications. A variable stiffness ply is denoted by <T> to distinguish it from a constant stiffness ply denoted by [θ]. The material properties of a typical graphite-epoxy composite from Jones [22] are listed in Table 1 and

used here. A quasi-isotropic (QI) laminate, $[45/0/-45/90]_{2s}$, with the same material is considered as the baseline for analysis. The reason behind this selection is that a QI design is used extensively in industries and is more robust than optimum CS laminates under various loading.

Table 1. Material properties of a typical graphite-epoxy composite [22].

Material Properties	Values			
E_1	30	msi	207	GPa
E_2	0.75	msi	5.17	GPa
ν_{12}	0.25		0.25	
G_{12}	0.375	msi	2.59	GPa
X_t	150	ksi	1.03	GPa
Y_t	6	ksi	41.4	MPa
X_c	100	ksi	689	MPa
Y_c	17	ksi	117	MPa
S	10	ksi	68.9	MPa

2.2. Modeling, analysis, and optimization

An optimal fiber path for a panel with discontinuity would be a continuous one that is steered around the cut-out [9-13, 15]. However, the methodologies used in [9-13, 15] were not able to generate continuous fibers across the panel and still resulted in breaks at the cut-out boundary. A unique approach to generate continuous curvilinear fiber paths with a single variable, i.e., initial ply angle, was introduced by the authors [20] using potential equations. Continuous curvilinear variable stiffness (CCVS) specimens were 3D printed, tested per ASTM D5766-11 for open-hole tensile strength, and compared with a constant stiffness (CS) design. The CCVS concept was further expanded in a later study to include geometries other than circular cut-outs [21]. A numerical technique known as “panel methods” was used in which a finite number of linear panels can be used to discretize an arbitrary geometry. The solution of the discretized panels is then able to generate the CCVS paths through the potential equations. It is worth mentioning that for defining fiber trajectories, there are other methods like linear functions [23], and many types of nonlinear functions, e.g., constant curvature path [24], B-Spline and Non-Uniform Rational Basis Spline (NURBS) hyper-surfaces [12, 13, 25], and Lobatto–Legendre polynomials [26], which have been studied in the literature. Although those functions offer a greater flexibility in defining a trajectory,

they need several parameters in their formulation. When a trajectory needs to be optimized for a large number of case studies, finding the optimal parameters requires numerous evaluations of the objective functions, which is computationally expensive. Hence, one significant benefit of the proposed panel method is that it requires only one parameter to define the trajectory for the entire ply. Another benefit of the proposed panel method is that the single parameter defines the complete set of fiber paths within a ply that are continuous and do not break at the cut-out boundary.

In this work, to obtain CCVS fiber paths, the circular cut-out was divided into 100 source panels. In addition, the square plates with the small (W/D = 2) and large (W/D = 4) holes were discretized into 1104 and 2000 elements, respectively. The source panel method was followed to find each source potential, Q, such that the superposition of the influence from other panels on each one has only a tangential component. Once the panel strength values were known, the fiber trajectory of any point on the square plates with cutouts can be found. It is the summation of influences of each panel on that point along with the contribution from the ply angle. A MATLAB subroutine was developed by the authors in the past [20, 21] and was used to calculate the trajectories for the two case studies. The examples of the fiber paths generated for the plate with a small hole for four different initial ply angles (IPA) can be seen in Figure 2.

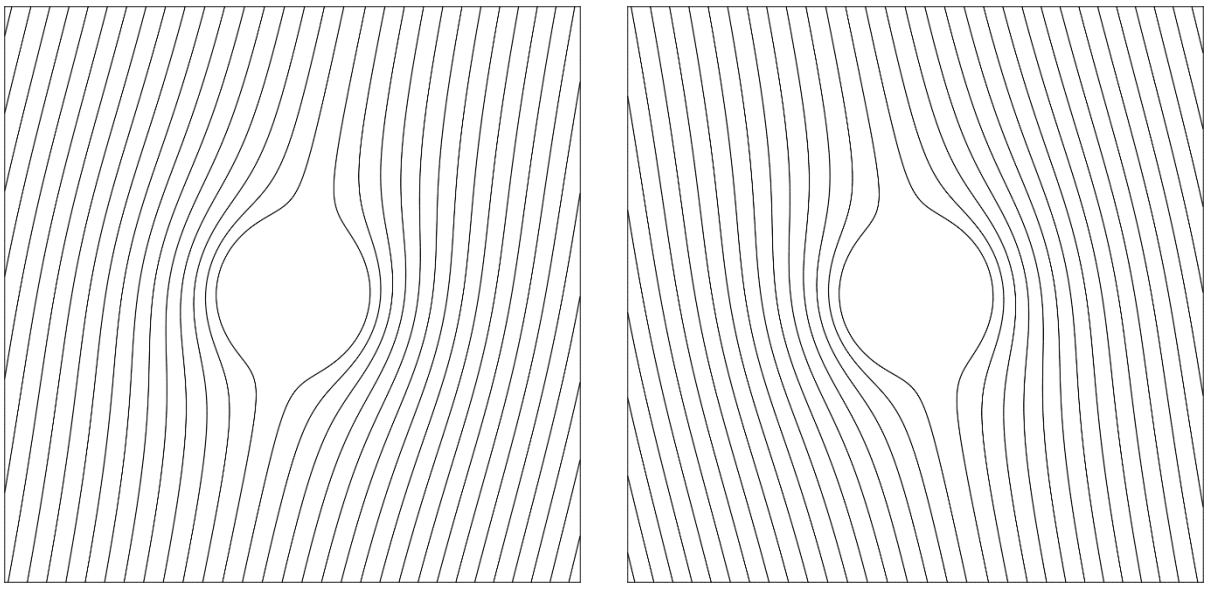

(a) **(b)**

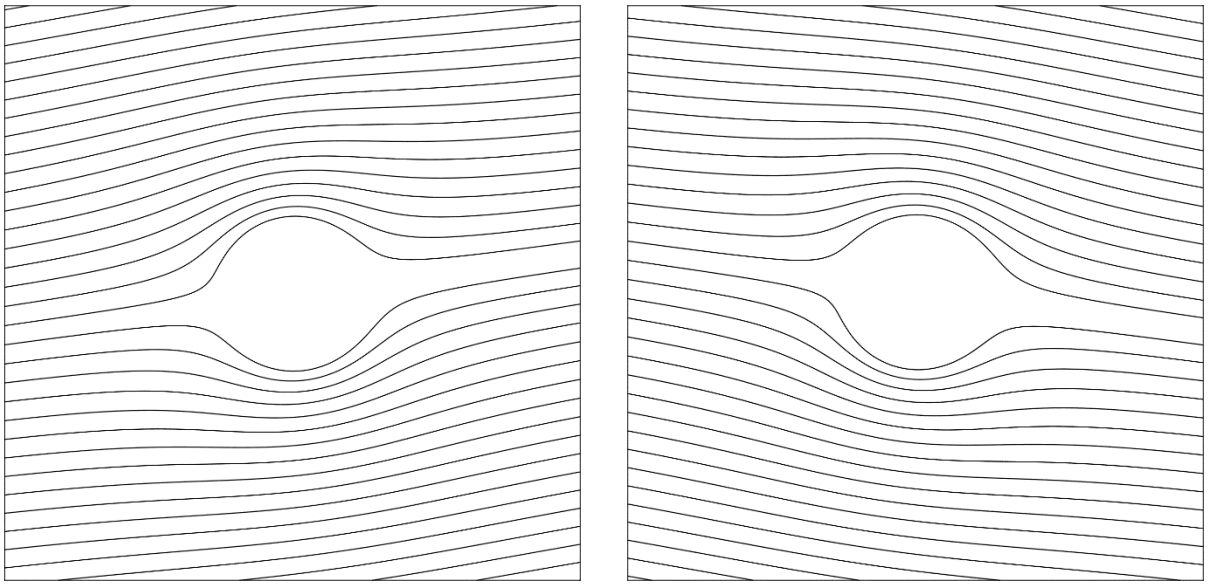

(c) **(d)**

Figure 2. Examples of continuous curvilinear fiber paths for a plate with a small hole at various ply angles: (a) ply <+78>; (b) ply <-78>; (c) ply <+8>; and (d) ply <-8>.

Figure 3 shows the flowchart for creating the finite element model of the case studies. The inputs are the initial ply angle and a matrix containing the element centroid coordinates, and the output is the computed fiber orientation angle, which is the tangent of the CCVS fiber path at the centroid of each element. It is assumed that the fiber angle is constant within each element and is equal to the value at the element centroid. In CCVS designs, the fiber orientation changes within the plane of the laminate as the fiber path follows a curvilinear trajectory; therefore, each element may have a different fiber angle and subsequently a different stacking sequence. Another MATLAB subroutine was developed in [21] to connect the CCVS fiber path generator and the FE solver. It extracts the element centroids from the FE mesh data and passes them to the CCVS fiber path generator to obtain fiber orientation at each element centroid. The process needs to be repeated through the thickness of the laminate since each layer might have a different IPA. Knowing the fiber orientation within each element and for all layers through its thickness, the MATLAB subroutine updates the PCOMP card (Layered Composite Element Property) for shell elements, which defines the element stacking sequence in the NASTRAN finite element model input file.

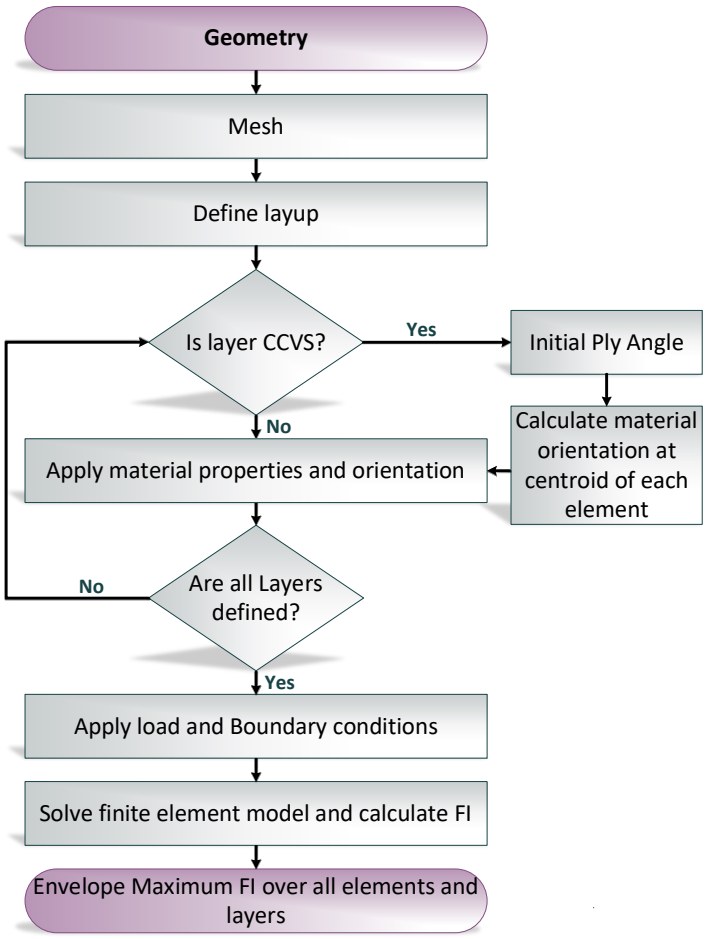

Figure 3. Flowchart for creating finite element model of case studies with CCVS design.

To eliminate the influence of mesh sizes in the generated finite element model, a convergence study is performed, and a plate is meshed with three different mesh sizes. The plate includes CCVS fiber paths with the IPA of 0° for all its plies and it is under uni-axial tension. Table 2 shows the element sizes around the hole, the corresponding number of elements, and the obtained Failure Index (FI) based on Tsai-Wu failure criterion. Model #2 has less than one quarter of elements for model #3 and this only resulted in 3 % difference in the FE result; therefore, model #2 is selected in this study for the FEA.

Table 2. Mesh Sensitivity analysis.

Model	Number of Elements	Elem. size around hole (mm)	Failure Index (FI)
1	1544	4.57	0.0127
2	2000	3.05	0.0131
3	8240	1.78	0.0134

First ply failure (FPF) method is used here to compare different designs by calculating the failure load per Tsai-Wu criterion. Since for CCVS design, the fiber angle changes spatially within the laminate, the failure index calculated by Tsai-Wu criterion will be different for each element through its thickness. Therefore, all elements need to be inspected to determine the FPF for the whole laminate. The goal is to find IPAs for a design that maximize the failure load; therefore, the optimization problem can be formulated as follows:

$$\max_{x}\{F(x)\}; x = (T_1, T_2, T_3, T_4)$$
$$s.t.\{T_1, T_2, T_3, T_4 \in [-90^{\circ}, +90^{\circ}]\} \quad (3)$$

, where **x** is the design variable vector, i.e., T_1 to T_4, the IPAs for each distinct ply, and F is the failure load. As mentioned in Section 2.1, stacking sequences of the CCVS laminates are denoted as $<\pm T_1/\pm T_2/\pm T_3/\pm T_4>_s$. Each CCVS ply is determined using only one IPA, i.e. T. As mentioned before, this notation is used to differentiate CCVS layup from the one with straight fibers, i.e. $[\pm\theta_1/\pm\theta_2/\pm\theta_3/\pm\theta_4]_s$. In this study, IPAs are considered as integers to respect the manufacturing accuracy of a typical AFP or a robotic 3D printer.

The optimization problem (Eq. 3) has several local optima since the design variables are ply angles. One can resort to two-level optimization techniques [13, 27], where lamination parameters are the design variable in first level and later in a second level a continuous fiber path resulting such laminate parameters are derived. Ghiasi et al [28, 29] reviewed multiple approaches including direct methods and multi-level techniques for optimizing variable stiffness composites. Evolutionary optimization algorithms, such as genetic algorithm (GA), are recommended to handle this type of design problems [30, 31]. GA optimization process might require thousands of function evaluations to locate a near optimal solution that makes the process computationally expensive. To alleviate the computational cost problem, one may resort to an approximation concept, also called a surrogate model, which is substituted and used in place of a finite element simulation. As a result, the metamodel can significantly reduce the time required to run the optimization. In this study, the Radial Basis Function surrogate model is used to find the optimum CCVS design for

each loading condition (a total of 40 optimization problems for each case study). For more details on the optimization method, the interested reader may refer to [32].

3. Results and discussions

3.1. CCVS designs under biaxial normal loading

Optimum CCVS designs for each loading condition were found (a total of 40 for each case study), where their failure load is the largest among their design counterparts. The optimum designs were obtained for the square plate with a large hole (W/D = 2, D = 7 in or 17.8 cm) and a small hole (W/D = 4, D = 3.5 in or 8.89 cm). To better visualize the results, failure load envelope based on the first ply failure theory for each plate is calculated, where the failure load is normalized with respect to the failure load of the QI layup under uniaxial tensile loading along x-axis. Figure 4 shows the failure load envelope for W/D = 2 and 4 cases for the CCVS designs and the QI layup. It should be noted that each CCVS design shown in Figure 4 has a different layup, which is the optimum layup for that biaxial loading combination and ratio, whereas the baseline remains as the QI layup. It is worth mentioning when loading is compressive, structural instability (buckling) may occur at lower load levels than material yielding. Buckling will be investigated in future studies to update the failure load envelopes presented in Figure 4.

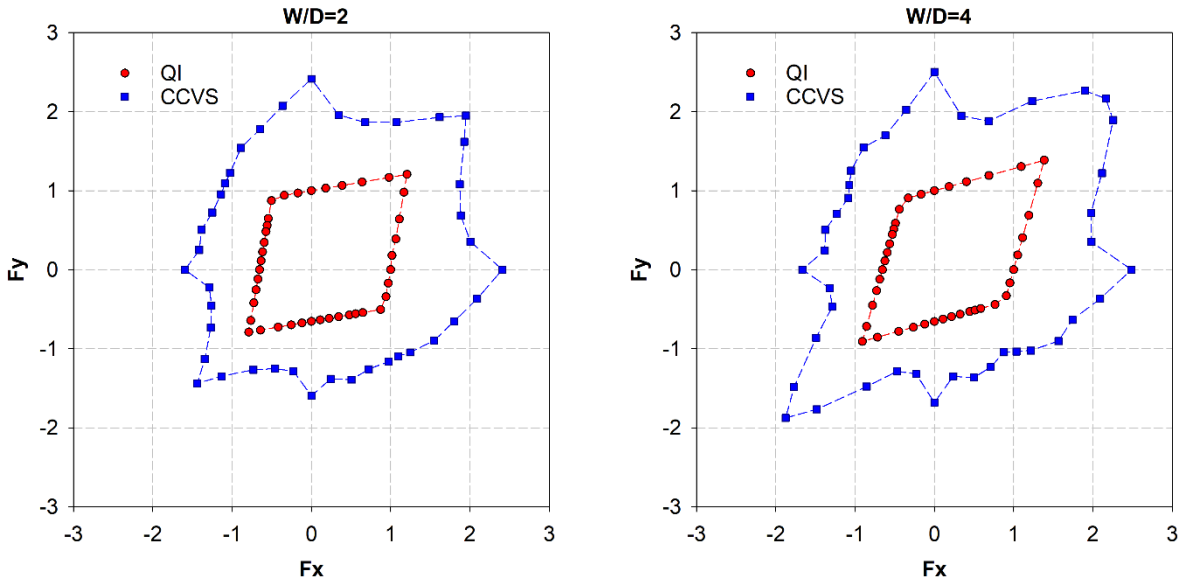

(a) **(b)**

Figure 4. Normalized first ply failure load for optimum CCVS design for each loading condition.

Per Figure 4, the failure load envelope of the QI layup takes the shape of a diamond, which is a characteristic of evaluating the laminate performance by the first ply failure procedure per Tsai-Wu criterion [33]. This also has been observed in the experimental data obtained by Huang et al. [34] for a QI laminate made from IM7-8552 with a circular cut-out under uni-axial tension, and T-T and T-C with equi-biaxial load ratios. For both cases, CCVS design increases the failure load for all biaxial loading ratios. This proves that CCVS design for a square plate with a cut-out is versatile and its improvement over the QI layup is not only limited to uniaxial loading conditions. This agrees with observation by other researchers as well who investigated biaxial tension loading for only one [12] and two force ratios [13, 15]. Such an improvement by CCVS design is expected since principal stress directions for any loading condition can be found, and by placing fibers along them, structural performance can be improved. The composite material investigated in this study has higher tensile strength along the fibers compared to the compressive strength (Table 1). Therefore, it is expected that the failure load envelope be shifted towards the first quadrant where both F_x and F_y loads are positive (tensile).

Figure 5 compares the normalized equivalent failure load of optimum CCVS designs at every biaxial loading combination and ratio. It can be seen that CCVS designs for both cases provide an improvement of at least 50 % in equivalent normalized failure load over the QI layup at any loading condition. The maximum improvement is achieved for uniaxial loading (either in tension or compression along x or y), i.e. β =0°, 90°, 180°, and 270°. As the loading condition deviates from uniaxial, the improvement in normalized equivalent failure load compared to the QI layup decreases, being minimum for the cases of T-T with equi-biaxial load ratios, β = 45°. The CCVS design for both plates with small and larger hole provided similar improvement in normalized equivalent failure load over QI layup with the notable exception for biaxial loadings which correspond to regions around equi-biaxial ratios of β = 45° (T-T), 135° (C-T), 215° (C-C), and 315° (T-C), where the square panel with a small hole generally performs better as it has more region around the hole to place the fibers.

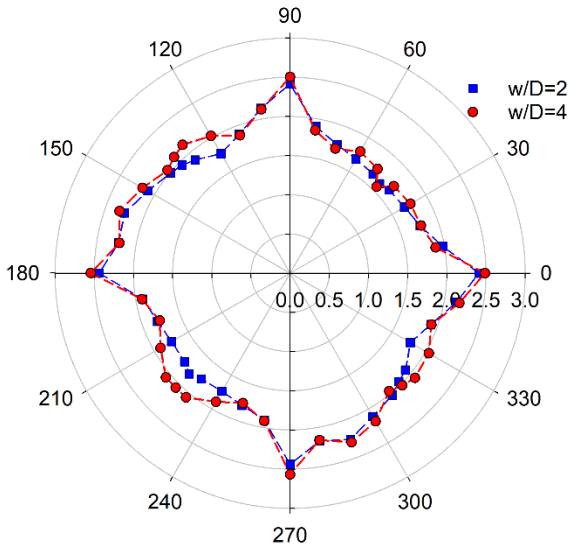

Figure 5. Improvement in normalized equivalent failure load using CCVS design over the QI layup for each biaxial loading combination and ratio, β.

3.2. CCVS panels under off-design conditions

It is recalled that each CCVS design shown in Figure 4 has its own layup optimized for the respected biaxial loading condition. To quantitively compare the improvement of a CCVS over a QI design, the following relative improvement factor is used:

$$I = \frac{F_{eq,CCVS}}{F_{eq,QI}} \tag{4}$$

, where $F_{eq,CCVS}$ is the equivalent failure load of a CCVS design, $F_{eq,QI}$ is the equivalent failure load of a QI design, and I is the improvement factor in the equivalent failure load. When there is an improvement in the equivalent failure load $I > 1$; on the other hand, $I < 1$ represents the case where the QI layup performs better than the optimum CCVS design. To evaluate the performance of each optimum CCVS design under off-design conditions, Figure 6 illustrates the improvement factor (I) of each of those CCVS designs at all biaxial loading combinations and ratios (β from 0° to 360°, the x-axis). Each row in Figure 6 indicates an optimum CCVS design labelled as CCVS-[β]. For example, CCVS-45 means the optimum CCVS layup that is obtained for maximum failure load under T-T equi-biaxial loading (β = 45°). The color bar value indicates the metric I. Since the requirement for a CCVS design is to provide a better or equal performance to a QI laminate,

in Figure 6, when a CCVS design does not provide an improvement over the QI layup ($I < 1$), then such a case is plotted with white color.

Figure 6 shows the performance of each optimum CCVS laminate in all loading conditions, i.e. per-design and off-design. The data along the diagonal of the Figure 6, from the bottom-left corner to the top right corner, corresponds to per design loading conditions plotted earlier in Figure 5. That is, where the loading ratio, β, is equal to the loading ratio used during the optimization of a CCVS design, CCVS-[β]. Per Figure 6, the maximum improvement in failure load is provided by designs optimized for uniaxial loading, i.e. CCVS-0, CCVS-90, CCVS-180, and CCVS-270 designs. However, they are the most sensitive layups to off-design conditions and their off-design performance diminishes significantly indicated by large regions of white spaces ($I < 1$). For the case of uniaxial loading, in regions away from the hole, optimum CCVS design has fibers within all plies along the loading direction, which makes it susceptible to loading in other directions (off-design conditions). It should be noted that this is also the case for optimum constant stiffness design (either $[0]_{24}$ or $[90]_{24}$), where the fibers within all plies are along the loading direction. The baseline here, a QI layup ($[45/0/-45/90]_{2s}$), while not optimum for uniaxial loading, is more robust than the optimum CCVS-[0] and CCVS-[90] designs under off-design conditions. It is worth mentioning that the optimization problem, Eq. (3), is formulated for a single objective, i.e. maximum failure load under a specified loading condition. Therefore, evaluating each of these optimum CCVS laminates at an off-design condition does not represent possible improvement from CCVS design over the QI layup. In the future, the authors will investigate formulating a multi-objective design problem to find the optimum CCVS design that will perform best in all off-design conditions. Nonetheless, among the presented CCVS designs, although not being the optimal for the off-design scenario, it can be seen that some of the CCVS designs are robust and considerably outperform the QI layup at all off-design conditions.

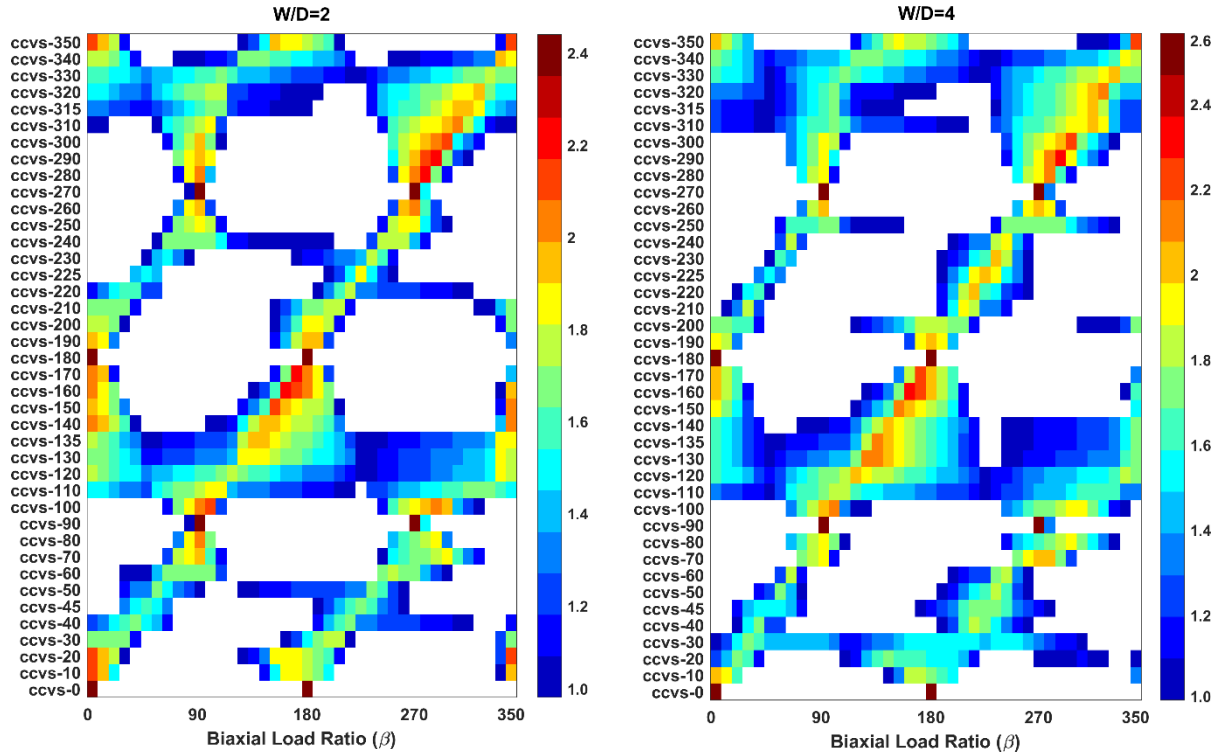

Figure 6. Improvement factor (*I*) of CCVS over the QI layup under all loading conditions.

To better assess the optimum CCVS designs under off-design conditions, Figure 7 shows their off-design coverage percentage and average improvement factor. The coverage percentage is the ratio of the number of off-design cases where the optimum CCVS design outperforms the QI design to the total number of cases, 40. The average improvement factor is the average of *I*, introduced in Eq. (4), for the cases where the optimum CCVS design outperforms the QI layup.

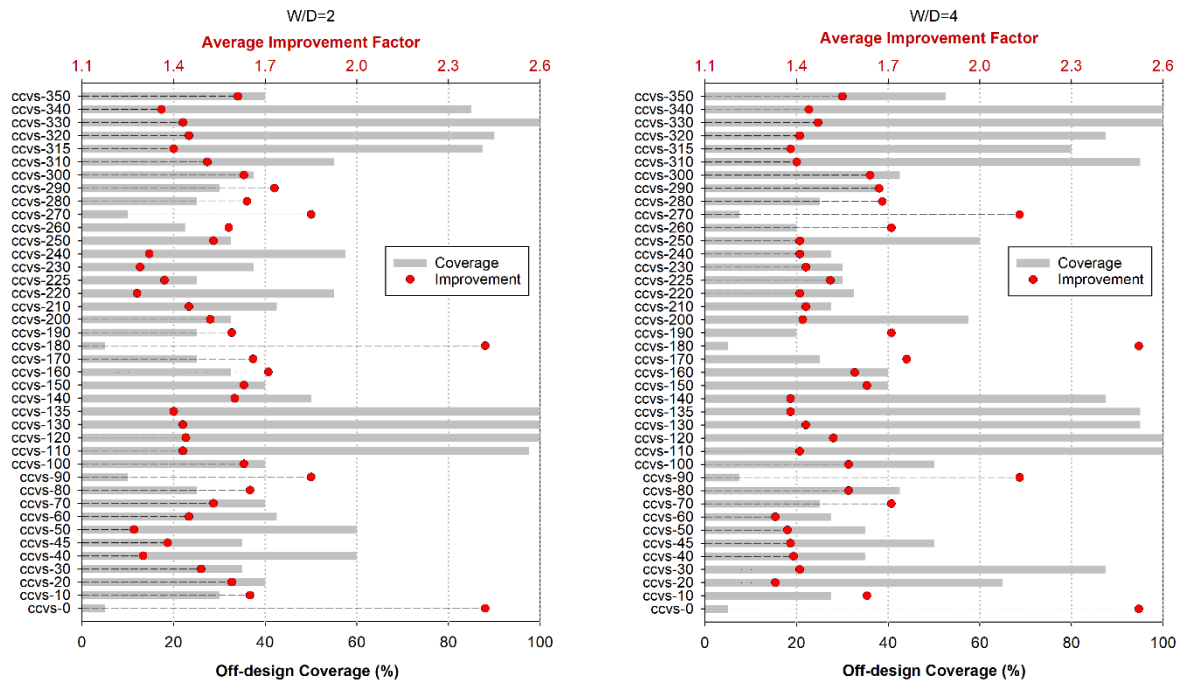

Figure 7. Effectiveness of optimum CCVS designs under off-design conditions.

In Figure 7, the averaged improvement factor, $\bar{I}$, identifies the effectiveness of a CCVS design and its robustness is determined by coverage percentage. For example, for the plate with a large hole (W/D = 2), CCVS-120, -130, -135, and -330 designs outperform the QI layup for all off-design conditions. This is CCVS-110, -120, -330, and -340 for the plate with a small hole (W/D = 4). Among all these designs, the CCVS-120 laminate has the highest average improvement over the QI layup for a plate with a large and a small hole, respectively, 52 % and 44 %. The stacking sequence of CCVS-120 for W/D=4 is $<\pm 78/\pm 8/\pm 78/\pm 8>_s$ and its continuous curvilinear fiber paths are illustrated in Figure 2 for the plate with a small hole.

Figure 8 shows the failure load envelope of the CCVS-120 design and the QI laminate for two case studies. It is clear that there is an improvement in failure strength of the CCVS-120 design compared to the QI laminate for any loading ratio. The failure location for a CCVS plate differs as the bi-axial normal loading combinations and their force ratio change. In a CCVS design, as opposed to a straight-fiber laminate, the fiber orientation varies spatially within the plane. Thus, the failure location for each applied loading might happen in a different element, which has a different stacking sequence. For the CCVS-120 design, as the bi-axial normal loading combination and its force ratio change, the on-axis stresses in the failed element vary. Per Figure 8, it can be observed that the quadratic combination of these on-axis stresses per Tsai-Wu criterion in the

failed elements remains almost constant for different loadings. Therefore, it can be concluded that the CCVS-120 design is insensitive to the biaxial loading combination and ratio. Considering a failure load component of F_x, a change in the F_y load component does not affect the magnitude of F_x and vice versa. Such a design will be beneficial for an application where the load in one direction is known while there might be changes in loading in the other direction. The optimum CCVS layup can be safely used based on only one component of the load capacity.

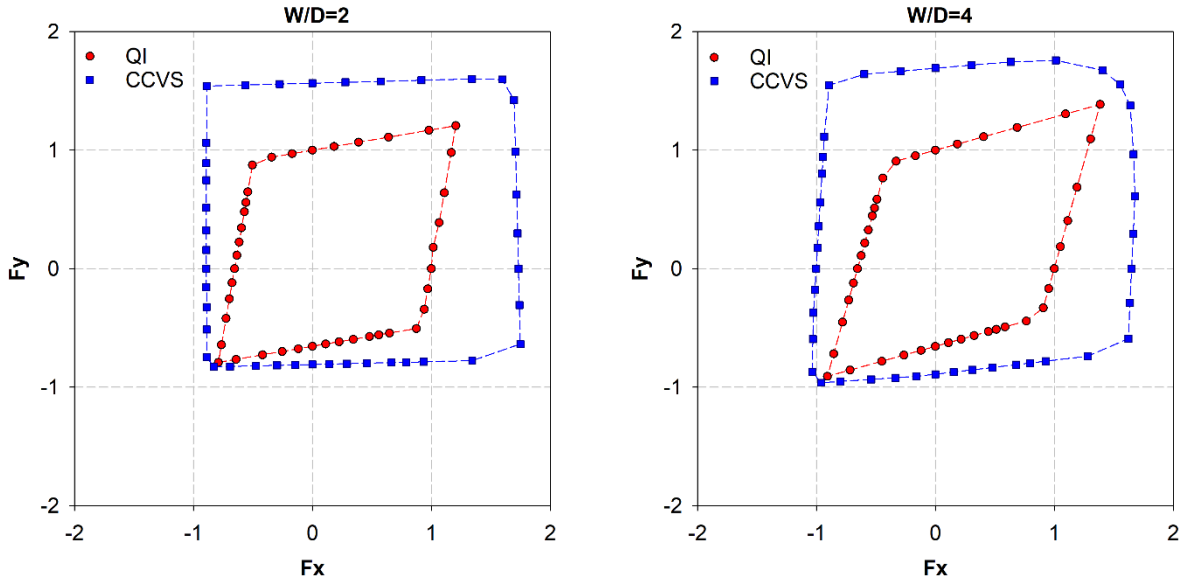

Figure 8: Normalized first ply failure load for CCVS-120 and the QI layup at all biaxial loading combinations and ratios.

Figure 9 shows the relative improvement, *I*, for the CCVS-120 design in all loading conditions compared to the QI layup. As expected, since CCVS-120 is the optimum design for the loading angle, β, of 120°, it provides a significant improvement there (I = 1.52 and I = 1.44 for plates with W/D=4 and W/D=2, respectively). The improvement in failure strength decreases for other loading angles, off-design conditions, with the exception of load ratios, β = 340° for case of W/D=2.

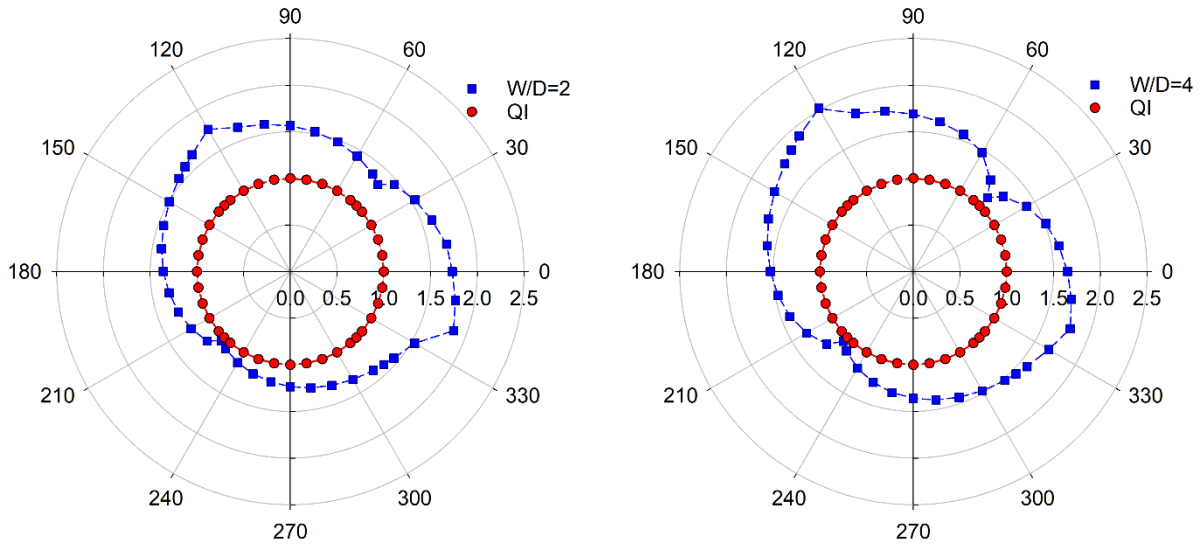

Figure 9. Improvement in the normalized equivalent failure load by CCVS-120 design over the QI layup for each biaxial loading combination and ratio, β.

The aim of this study is to demonstrate the load carrying capacity of CCVS designs under various biaxial normal loading and their force ratios. When one or both normal loadings are compressive, buckling failure might become a design factor. It should be mentioned that for such a case, the buckling load can be added as another objective to optimization formulation to obtain a design that satisfy all required design criteria [32, 35], which will be the subject of a future study. Here, the buckling load of the optimum design with W/D=4 under uni-axial compression along x-direction (CCVS-180) and equi-biaxial compressive load ratios (CCVS-225) is investigated. Table 3 shows the buckling load of the two selected designs normalized with that of quasi-isotropic laminate (baseline). The buckling load capacity of the CCVS-180 is degraded by about 24%, whereas the buckling load capacity of the CCVS-225 is improved significantly by 49%. From Figure 9, it can be seen that CCVS-225 has a similar compressive load failure as the QI, but its buckling load capacity is considerably improved.

Table 3. Normalized buckling load for a plate with a small hole.

Design	Normalized buckling load
CCVS-180	0.76
CCVS-225	1.49

4. Conclusions

In conclusion, continuous curvilinear variable stiffness (CCVS) designs were explored to improve strength of a square plate with a circular hole compared to a quasi-isotropic laminate, the baseline. The panel methods and the potential equations were used to generate the CCVS paths for plates with two different hole diameters. MATLAB subroutines were developed to build finite element model of CCVS designs knowing their fiber orientation through the thickness. First ply failure (FPF) load per Tsai-Wu criterion was used as the objective function in an optimization problem to find optimum stacking sequence for CCVS designs. Biaxial normal loading with all possible combinations and multiple force ratios were investigated (a total of 40 optimization problems for each case study). CCVS designs for both cases provided at least 50 % improvement in failure load compared to the baseline at any biaxial normal loading condition. Optimum CCVS designs were then subjected to off-design loading and their strength was compared with the baseline (39 off-design loading for each design). As expected, CCVS designs optimized for uniaxial loading were extremely sensitive to off-design loading and their performance was lower than the baseline for almost all off-design loading conditions. Interestingly, there were optimum CCVS designs that performed better than the baseline at all off-design loading conditions. For example, the CCVS-120 laminate exhibited an average improvement of 52 % and 44 % compared to the baseline for the plate with a large and a small hole, respectively. They are insensitive to biaxial loading combinations and force ratios, which makes them very practical for applications where the part loading might change during service.

Robotic 3D printing and biaxial testing capabilities currently in development at the Facility for Research on Aerospace Materials and Engineered Structures (FRAMES) at Ryerson University can accommodate plates up to 15 in × 15 in (38.1 cm × 38.1 cm). Maximum curvature or minimum turning radius of fiber paths imposed by the robotic 3D printing technique will be evaluated based on the process parameters, material type, and the tow width. This fabrication constraint will be considered in the optimization process to ensure manufacturability of optimum designs. Several optimum CCVS designs in tension-tension loading combination will be manufactured and tested to validate the numerical results. In-process inspection by a laser line scanner will be used to characterize defects (e.g., gaps) induced in the laminates during 3D printing. The impact of gaps on the strength of CCVS laminates will be explored to accurately evaluate their performance compared to straight-fiber laminates.

Data availability

The raw/processed data required to reproduce these findings cannot be shared at this time as the data also forms part of an ongoing study.

Declaration of Competing Interest

The authors declare that there are no conflicts of interest.

References

[1] Lopes, C.S., Gürdal, Z. and Camanho, P.P., 2008. Variable-stiffness composite panels: Buckling and first-ply failure improvements over straight-fibre laminates. Computers & Structures, 86(9), pp.897-907.

[2] Megson, T.H.G., 2016. Aircraft structures for engineering students. Butterworth-Heinemann.

[3] Jegley, D., Tatting, B. and Gurdal, Z., 2003, April. Optimization of elastically tailored tow-placed plates with holes. In 44th AIAA/ASME/ASCE/AHS/ASC Structures, Structural Dynamics, and Materials Conference (p. 1420).

[4] Wu, K.C., Turpin, J.D., Gardner, N.W., Stanford, B. and Martin, R.A., 2015. Structural characterization of advanced composite tow-steered shells with large cutouts. In 56th AIAA/ASCE/AHS/ASC Structures, Structural Dynamics, and Materials Conference (p. 0966).

[5] Alhajahmad, A., Abdalla, M.M. and Gürdal, Z., 2008. Optimal design of a pressurized fuselage panel with a cutout using tow-placed steered fibers. in International confrence on engineering optimization, Rio de Janeiro, 2008.

[6] Lopes, C.S., Gürdal, Z. and Camanho, P.P., 2010. Tailoring for strength of composite steered-fibre panels with cutouts. Composites Part A: Applied Science and Manufacturing, 41(12), pp.1760-1767.

[7] Yau, S.S. and Chou, T.W., 1988, January. Strength of woven-fabric composites with drilled and molded holes. in Composite Materials: Testing and Design (Eighth Conference), ed. J. Whitcomb (West Conshohocken, PA: ASTM International, 1988), 423-437. https://doi.org/10.1520/STP26150S

[8] Durante, M. and Langella, A., 2009. Bearing behavior of drilled and molded-in holes. Applied Composite Materials, 16(5), pp.297-306.

[9] Hyer, M.W. and Lee, H.H., 1991. The use of curvilinear fiber format to improve buckling resistance of composite plates with central circular holes. Composite structures, 18(3), pp.239-261.

[10] Huang, J., and Haftka, R. 2005. Optimization Design of Composite plates with holes for increased strength. Struct Multidisc Optim (2005) 30: 335-341. DOI 10.1007/s00158-005-0519-z

[11] Gustafson, P. and Gustafson, P., 2011. Fiber tailoring for durability improvement of bolted composite plates. In 52nd AIAA/ASME/ASCE/AHS/ASC Structures, Structural Dynamics and Materials Conference 19th AIAA/ASME/AHS Adaptive Structures Conference 13t (p. 2047).

[12] Montemurro, M. and Catapano, A., 2019. A general B-Spline surfaces theoretical framework for optimisation of variable angle-tow laminates. Composite Structures, 209, pp.561-578.

[13] Catapano, A. and Montemurro, M., 2020. Strength Optimisation of Variable Angle-Tow Composites Through a Laminate-Level Failure Criterion. Journal of Optimization Theory and Applications, 187(3), pp.683-706.

[14] Catapano, A. and Montemurro, M., 2019. On the correlation between stiffness and strength properties of anisotropic laminates. Mechanics of Advanced Materials and Structures, 26(8), pp.651-660.

[15] Shafighfard, T., Demir, E. and Yildiz, M., 2019. Design of fiber-reinforced variable-stiffness composites for different open-hole geometries with fiber continuity and curvature constraints. Composite Structures, 226, p.111280.

[16] Catapano, A., Desmorat, B. and Vannucci, P., 2015. Stiffness and strength optimization of the anisotropy distribution for laminated structures. Journal of Optimization Theory and Applications, 167(1), pp.118-146.
[17] Rouhi, M., Ghayoor, H., Hoa, S.V. and Hojjati, M., 2015. Multi-objective design optimization of variable stiffness composite cylinders. Composites Part B: Engineering, 69, pp.249-255.
[18] Jegley, D., Tatting, B. and Gurdal, Z., 2005, April. Tow-steered panels with holes subjected to compression or shear loading. In 46th AIAA/ASME/ASCE/AHS/ASC Structures, Structural Dynamics and Materials Conference (p. 2081).
[19] Gomes, V.S., Lopes, C.S., Pires, F.F.A., Gürdal, Z. and Camanho, P.P., 2014. Fibre steering for shear-loaded composite panels with cutouts. Journal of Composite Materials, 48(16), pp.1917-1926.
[20] Khan, S., Fayazbakhsh, K., Fawaz, Z. and Nik, M.A., 2018. Curvilinear variable stiffness 3D printing technology for improved open-hole tensile strength. Additive Manufacturing, 24, pp.378-385.
[21] Khan, S., Arian Nik, M., Fayazbakhsh, K. and Fawaz, Z., 2020. Continuous curvilinear variable stiffness design for improved strength of a panel with a cutout. Mechanics of Advanced Materials and Structures, pp.1-9.
[22] Jones, R.M., 1998. Mechanics of composite materials. CRC press.
[23] Gurdal, Z. and Olmedo, R., 1993. In-plane response of laminates with spatially varying fiber orientations-variable stiffness concept. AIAA journal, 31(4), pp.751-758.
[24] Blom, A.W., Lopes, C.S., Kromwijk, P.J., Gurdal, Z. and Camanho, P.P., 2009. A theoretical model to study the influence of tow-drop areas on the stiffness and strength of variable-stiffness laminates. Journal of composite materials, 43(5), pp.403-425.
[25] Audoux, Y., Montemurro, M. and Pailhès, J., 2020. A metamodel based on non-uniform rational basis spline hyper-surfaces for optimisation of composite structures. Composite Structures, 247, p.112439.
[26] Alhajahmad, A., Abdalla, M.M. and Gürdal, Z., 2008. Design tailoring for pressure pillowing using tow-placed steered fibers. Journal of aircraft, 45(2), pp.630-640.
[27] Fiordilino, G.A., Izzi, M.I. and Montemurro, M., 2021. A general isogeometric polar approach for the optimisation of variable stiffness composites: Application to eigenvalue buckling problems. Mechanics of Materials, 153, p.103574.
[28] Ghiasi, H., Fayazbakhsh, K., Pasini, D. and Lessard, L., 2010. Optimum stacking sequence design of composite materials Part II: Variable stiffness design. Composite structures, 93(1), pp.1-13.
[29] Ghiasi, H., Fayazbakhsh, K., Pasini, D. and Lessard, L., 2010. Optimum stacking sequence design of composite materials Part II: Variable stiffness design. Composite structures, 93(1), pp.1-13.
[30] Park, J.H., Hwang, J.H., Lee, C.S. and Hwang, W., 2001. Stacking sequence design of composite laminates for maximum strength using genetic algorithms. Composite Structures, 52(2), pp.217-231.
[31] Nagendra, S., R.T. Haftka, and Z. Gürdal, Genetic Algorithms for the Design of Composite Panels, in Advanced Technology for Design and Fabrication of Composite Materials and Structures: Applications to the Automotive, Marine, Aerospace and Construction Industry, G.C. Sih, A. Carpinteri, and G. Surace, Editors. 1995, Springer Netherlands: Dordrecht. p. 129-143.
[32] Nik, M.A., Fayazbakhsh, K., Pasini, D. and Lessard, L., 2014. A comparative study of metamodeling methods for the design optimization of variable stiffness composites. Composite Structures, 107, pp.494-501.
[33] Richard M. Christensen, The Theory of Materials Failure, Oxford University Press, Oxford, 2013.

[34] Huang, Y., Ha, S.K., Koyanagi, J., Melo, J.D.D., Kumazawa, H. and Susuki, I., 2010. Effects of an open hole on the biaxial strengths of composite laminates. Journal of composite materials, 44(20), pp.2429-2445.
[35] Nik, M.A., Fayazbakhsh, K., Pasini, D. and Lessard, L., 2012. Surrogate-based multi-objective optimization of a composite laminate with curvilinear fibers. Composite Structures, 94, pp. 2306-2313.